

Non-uniform illumination representation based on HDR light probe sequences

Jian Hu, Tao Yu, Lin Wang, Zhong Zhou*, Wei Wu
State Key Laboratory of Virtual Reality Technology and Systems
Beihang University
Beijing, China
**Email: zz@vrlab.buaa.edu.cn*

Abstract

This paper presents a method to represent the complicated illumination in the real world by using HDR light probe sequences. The illumination representations proposed in this paper employ non-uniform structure instead of uniform light field to simulate lighting with spatial and angular variation, which turns out to be more efficient and accurate. The captured illuminations are divided into direct and indirect parts that are modeled respectively. Both integrated with global illumination algorithm easily, the direct part is organized as an amount of clusters on a virtual plane, which can solve the lighting occlusion problem successfully, while the indirect part is represented as a bounding mesh with HDR texture. This paper demonstrates the technique that captures real illuminations for virtual scenes, and also shows the comparison with the renderings using traditional image based lighting.

Keywords: light field; non-uniform representation, high dynamic range imaging, image based lighting

1. Introduction

Recently, numerous researchers have been involved to illuminate the virtual scenes using the illuminations captured from real scenes to produce the photo-realistic rendering. Considering huge amounts of the illumination data as well as the high-dimensional feature, it is significant to construct the raw illumination data into some representations, which can be easily integrated into the realistic lighting algorithm framework.

A lot of novel and practical illumination capturing setups have been proposed in previous work, and all of them produced massive data which is quite difficult to be directly used for rendering. The illumination in the real-world is high-dimensional, and modeled as the 7D function $I = f(x, y, z, \theta, \varphi, \lambda, t)$ by early researchers. The regular approach reduces this function to 3D or 4D, and captures the spatially and angularly varying illumination based on this simplified version. Yet these methods are all

struggled to determine the size of the sampling density, which is related to the efficiency and accuracy.

Based on the 2D HDR angular map of the environment sequence, i.e. light probe sequence, we construct a non-uniform data structure to represent the direct illumination incident to the real scene. This structure keeps the different density of light sample pair with different lighting variations. And we employ a scene-based bounding mesh to represent the rest indirect illumination, which provide lots of vision cues. Finally, we discuss the capturing strategy on shortening the lighting capturing time using adaptive sampling methodology.

The rest of the paper is organized as the following: In section 2, the related work is introduced. Section 3 describes the non-uniform illumination representations in detail. The integration of the non-uniform representations to current realistic illumination algorithm is presented. In section 4, the capturing setup and its data processing procedure are introduced. The experimental results are shown in section 5, where performance and the limitations of the proposed method are analyzed.

2. Related Work

Complicated modeling of the real-world light source can greatly improve the realism of synthetic images. Heidrich et al. [1] first proposed a discretized vision of light field to store the illumination from light sources for virtual object rendering. Built on the same idea, this paper employs non-uniform structure to gain higher precision and efficiency. Goesele M. et al. [2] presented two kinds of setups that captured the illumination distribution from light sources and then integrated them into the canned light source to illuminate the virtual scene. However, the acquisition process could turn out more efficient by using the translation stage instead of manual drive. Recently, Mas A. et al. [4] introduced a method that the light sources are represented as numerous discretized rays on a triangular mesh. The data is compressed dramatically, yet the directional distribution is further improved.

A number of capturing devices have been proposed to acquire the illumination incidents as to area or volume, and the data is used to build representations that depict the

incident light field [5]. Unger J. et al. [6] brought up two new devices for the acquisition of spatially varying illumination. In particular, a specific rendering procedure using the data obtained directly was developed. However, the capturing time turned out to be the main limitation for practical applications. Without further abstraction, it is difficult to integrate the captured data into the current rendering framework. J. Low et al. [8] reconstructed the incident light field on a spherical harmonic grid, yet the sample density and distribution limited the spatial and angular resolution of the uniform grid. Mury A.A. et al. [9] simplified the light field structure and put forward a method for reconstruction of the light field in finite space.

Some researchers studied the real illumination reconstruction from other perspectives. Sato I. et al. [10] found a correlation between irradiance on the image plane and that on the surface of real objects, and reconstructed an approximate radiance distribution on geometry mesh. In his paper, an approximate geometry of real scene is obtained by using two omni-directional images captured in different positions. Corsini M. et al. [11] introduced a practical method to estimate the position, shape, and intensity of real light sources in the real scene with illuminations captured by two mirror balls. Y. Furukawa et al. [12] presented a novel multi-view stereo approach to reconstruct the geometry of a real scene, which can be used for illumination representation in this paper. The illumination can also be used to help color calibration as our previous work [13].

Considering the efficiency and accuracy of the light field representation, some non-uniform approaches have been presented. Ihrke I. et al. [3] proposed to use an inexpensive mirror to obtain non-uniform illumination data. However the data was resampled to a Lumigraph for rendering. And Unger, J. et al. [7] presented an irregular 4D ray representation for illumination with a certain bounding volume. The spatial distribution is represented in a non-uniform structure, while the angular distribution is still recorded on a uniform grid, a limitation to resampling.

Inspired by the approaches above for light source modeling and incident light field representation, this paper aims to propose an algorithm to represent the real illumination in the elaborate structure, and relevant data acquisition and processing is introduced. Different from the traditional uniform light field structure, our proposal employ non-uniform structure to model the real illumination distribution. Moreover, it is easier to integrate the representation with the realistic rendering framework. For data acquisition, Unger J. et al. [6]’s high fidelity incident light field capturing device is employed to capture a spatially-varying illumination in our experiment, and the problem of a tedious capturing time is solved through the performance of an adaptive capturing on the plane.

3. Illumination Representations

In this section we introduce the structures to represent illumination distribution using the lighting information capturing from the real world. The light capturing device we will use is motivated by Unger J. et al. [6]’s high fidelity incident light field device which can obtain the light probes from different positions distributed on a plane. For each light probe captured at a certain position (\mathbf{u}, \mathbf{v}) , it contains the lighting incident from different directions (θ, φ) . Based on the photographed light probe sequence, we can represent the illumination in the real-world with elaborately designed structure, and this is integrated with the global illumination algorithm to generate a realistic rendering result.

In order to lower the variance in the final rendering image, importance sampling is always employed to estimate the lighting of the point on the plane. Like the light probe sampling in the image based lighting, the area with different intensity must be sampled with different density. So we divide the illumination into direct and indirect parts according to the lighting intensity and employ different structures to represent them respectively.

3.1. Direct Illumination

For each light probe L_p captured at a certain position (\mathbf{u}, \mathbf{v}) , it contains the lighting incident from different directions (θ, φ) . So L_p can be seen as a set of sample rays from all directions to a single point. The light probe sequences can be represented as a set of rays, equation 1.

$$\mathbf{R} = \{\mathbf{r} \mid \mathbf{r} = \mathbf{f}(\mathbf{u}, \mathbf{v}, \theta, \varphi)\} \quad (1)$$

Based on this, the rays belonging to direct illumination can be recorded as $\mathbf{R}^{\text{direct}}$. By analyzing the similarity of the rays’ spatial and angular property, the direct illumination also can be classified into different groups. For each group of rays, the discrete representative ray samples distributed on a virtual plane are employed to simulate the real illuminants.

3.1.1. Direct Illumination Division. Firstly we construct a virtual plane, which is initially paralleled to the capturing plane, to divide the direct illumination rays’ set into different groups. Each group holds the rays which have the similar spatial and angular property. By projecting the rays onto the plane, the 4D rays are converted to 2D points. And we employ the hierarchical clustering algorithm on the points to divide the rays into different clusters.

As Figure 1(a) shows, we firstly place a virtual plane L_v at the initial position within the camera lens height \mathbf{h}_0 . Then each ray in set $\mathbf{R}^{\text{direct}}$ is projected onto L_v and intersected with it on the coordinate of $\mathbf{p}(x', y', \mathbf{h}_0)$. With the changing of the height of virtual plane, the distribution of intersections will be rearranged correspondingly. We

apply a hierarchical clustering algorithm on this two-dimensional point cloud to generate several clusters with partial points. For each cluster C_i , we make use of the objective function shown as equation 2 to obtain a value which represents the dispersion degree of the points in C_i . The optimal position of the virtual plane can be established when objective function achieves minimum.

$$f(\mathbf{h}_i) = f_{\text{area}}(f_{\text{cluster}}(\bigcup_{i=1}^n \mathbf{p}_{(i, \mathbf{h}_i)})) \quad (2)$$

where $\mathbf{p}_{(i, \mathbf{h}_i)}$ stands for the intersection of rays in $\mathbf{R}^{\text{direct}}$ and the L_v at a certain height \mathbf{h}_i . f_{cluster} is a function that distribute the intersections into different clusters C_i according to distance, and f_{area} calculates the area of convex hull of the intersections in each C_i . Figure 1(b) indicates the gradual change of the distribution of the intersections on the virtual plane as the plane moves vertically. It's clear that the left cluster decreases into a small intensive area from a large sparse area.

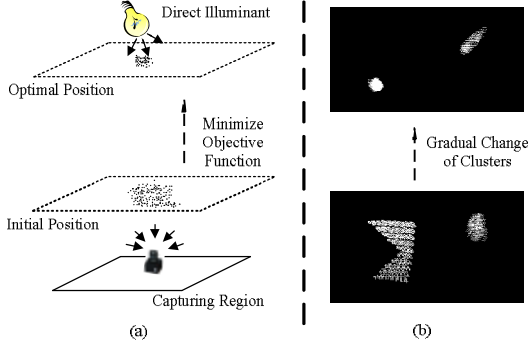


Figure 1. Virtual Plane Estimation. (a) Process to move the virtual plane to the optimal position (b) Gradual change of the cluster along with the movement of virtual plane

Finally, each cluster C_i will be placed at the optimized position by minimizing the objective function. Our direct illumination structure only records the rays with similar property, but not corresponds with the real light source in the real scene, which has little influence on the later global illumination rendering, because all structures hold the full ray samples. Consequently, this representation of direct illumination can well simulate complex light sources in the real scene.

3.1.2. Sample Ray Structure. As we have established an optimal position of the virtual plane L_v , and the rays in $\mathbf{R}^{\text{direct}}$ are distributed into each L_v . Then we need to construct these rays into the sample ray non-uniform structure Γ , which is convenient for resampling. Specifically, we select a certain amount of representative points within the intersections' convex hull, and each representative point \mathbf{p}_r represents the rays with their intersections within the neighborhood of \mathbf{p}_r . Figure 2 shows the structure we presented to construct the rays.

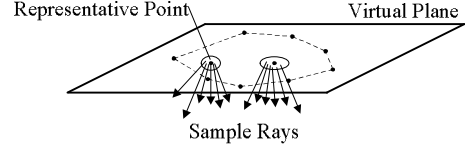


Figure 2. Non-uniform structure for ray samples

The construction of the non-uniform structure Γ from chaotically spreading rays is as the following:

1. If the $\mathbf{R}_i^{\text{direct}}$ is not vacant; select one ray \mathbf{r}_i from it with its intersection (x_0, y_0) , and add it to a new representative point \mathbf{p}_r which is placed at the initial coordinate (x_0, y_0) .
2. Find the nearest intersection to \mathbf{p}_r in $\mathbf{R}_i^{\text{direct}}$ and add it to \mathbf{p}_r if the new point is in the neighborhood of the position of \mathbf{p}_r .
3. Recalculate the position of representative point by equation 3.

$$\mathbf{p}(\bar{x}, \bar{y}) = \frac{1}{N} \sum_{i=1}^N (x'_i, y'_i) \quad (3)$$

Then repeat step 2 until no ray can be appended and then go to step 1 until the set $\mathbf{R}_i^{\text{direct}}$ is empty. Having the representative points distributed on the plane, we use Delaunay Triangulation to partition the virtual plane with representative points as vertexes of the triangles.

In the real-world, the directional and spatial distribution of illumination is not always uniform, so the uniform sampling of the incident light field leads to an amount of redundant data that can be filtered. Based on this, our idea is that if the sample rays have little influence on the interpolation of the unknown ray, we can drop it, as Figure 3 indicates the procedure of dropping sample ray \mathbf{p}_4 .

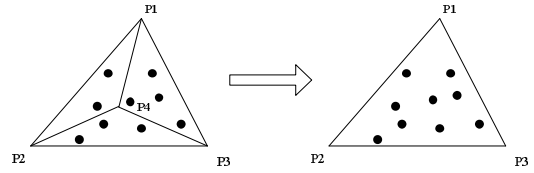


Figure 3. Sample Point Decimation Test

If we want to check whether \mathbf{p}_4 can be disposed, firstly find a polygon $\langle \mathbf{p}_1, \mathbf{p}_2, \mathbf{p}_3 \rangle$ surround \mathbf{p}_4 , then randomly choose server rays in the polygon and resample their light intensity with and without \mathbf{p}_4 . If their difference is lower than the threshold, consider \mathbf{p}_4 is discardable.

3.1.3. Direct illumination resampling. The direct illumination representation records the lighting samples in a non-uniform structure, and then the key point is how to obtain arbitrary lighting information by interpolation of the existed samples. The ray resampling process is described in Figure 4.

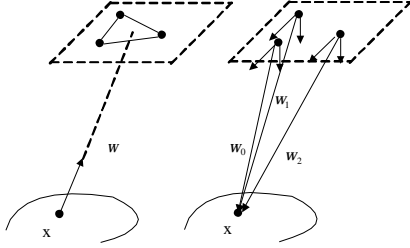


Figure 4. Direct illumination representation resampling

When computing the direct lighting of \mathbf{x} in direction ω , we can construct one ray starting from point \mathbf{x} in direction ω and project it onto one virtual plane with an intersection $(\mathbf{x}', \mathbf{y}')$. For the virtual plane that is partitioned by Delaunay Triangulation, there will be one triangle that the point $(\mathbf{x}', \mathbf{y}')$ belongs to. Each triangle vertex on the virtual plane records several sample rays projecting in various directions. So firstly we need to find the nearest rays, calculate the value of the 3 rays from the 3 vertices to point \mathbf{x} , and the directions of the 3 rays are $(\omega_1, \omega_2, \omega_3)$. Then we use the triangular interpolation to resample the value of the ray (\mathbf{x}, ω) .

3.2. Indirect Illumination

Indirect illumination plays an important role in displaying the photo-realistic effect of lighting. By constructing the approximate geometry of the scene and radiance distribution on it, we simulate the indirect illumination as a luminous bounding geometry.

In order to construct the geometry of the real scene, we firstly recover the position of feature points in the space. Every two light probes overlap largely. So knowing the light probes' capturing positions, we can easily recover the positions of the feature points in space by stereo vision. Then a 3D triangulation algorithm can be applied directly to establish the 3D triangular mesh of the real scene. For two light probes I_1 and I_2 , we employ the Harris and DOG operator to extract amount of feature points. We connect the optical centers and matching feature points, then two rays are formed. The intersection of the two rays is the restored position.

After constructed the approximate geometry of the scene from light probe sequence, we use the spherical projection recover the radiance distribution on the triangle mesh. SATO I. et al. [10] derive the relationship between the irradiance on the image plane and the radiance on the object surface in the scene in Equation 4

$$E = L \frac{\pi}{4} \left(\frac{d}{f}\right)^2 (1 + \theta^2)^2 \cos^3(\tan^{-1} \theta) \cos \theta \quad (4)$$

where L is the radiance of the light source and E represents the corresponding irradiance on the image plane. The equation can be directly used in our application to project the omni-directional image onto the approximate geometry of the scene. The values of the rays

can be resampled by the lighting intensities of the intersections of rays and the indirect illumination structure.

4. System Overview based on the Non-Uniform Representation

In this section, the work flow from illumination data capturing to non-uniform representation rendering are depicted in detail in the following subsections.

4.1. Capturing Setup

We build the setup similar to that in [6] to capture the illumination incident to a plane in the real-world. The setup contains panoramic camera, 2-dimensional translation stage, and control system that control the moving of stage and camera photographing. The translation stage which supports the panoramic camera can perform a movement in the range of $500 * 500$ with maximum error 0.01. We use PointGray's Ladybug3 panoramic camera, with a maximum resolution of $2048 * 2048$ pixels, which can conveniently capture the illumination in a wide angle. At each capturing position, 8 images are captured with different exposure time from $1/256$ of a second to 1 second (Figure 5) to combine the high dynamic range light probes by recovering the response curve [15].



Figure 5. Image series for light probe fusion

For the panoramic camera is pre-calibrated internal, we can use the virtual ideal spherical image sensor model. That is we suppose there is a unit sphere located at the common optic centre of the panoramic camera, and the captured images can be mapped onto the sphere surface as shown in Figure 6. The connection of optic centre and the arbitrary point P at space will intersect the sphere on p which is represented by the spherical coordinate (θ, φ) .

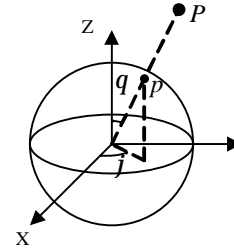


Figure 6. Spherical image and spherical projection

4.2. Adaptive Capturing Strategy

The distribution of real illumination is complicated spatially and angularly. The capturing strategy, uniform sampling on the plane can be a waste of time. For the highly varying area of the illumination, intensive sampling can precisely represent the distribution feature. And the area with invariant illumination has no need for the too much samples. Here we figure out a strategy to take an adaptive capturing spatially, which alleviate the problem. After installing the capturing setup in the specific environment, we firstly place a diffuse white board above the panoramic camera horizontally. Then we mark the area corresponding to capturing range below and take photo of the board from upside.

The image indicates radiance distribution on the capturing plane. We can take advantage of this distribution to arrange the capturing position on the plane instead of uniform capturing on the grid. In this paper, we try to extract the gradient of the image and take more samples in the area with higher gradient.

4.3. Direct Illumination Extraction

Since the direct and indirect illuminations are represented in different structure, it is necessary to segment the initial light probe into direct and indirect parts. In each light probe, the direct illumination area has the value orders of magnitude larger than indirect area because of the HDR feature. Here the energy histogram of light probes is applied in segmentation.

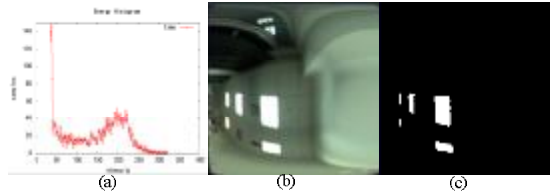


Figure 7.(a) Energy histogram of light probes (b) Initial light probe (c) Partitioned result of the light probe

As the Figure 7 (a) shown, the horizontal axis stands for the light intensity, and vertical axis represents the count of the samples. The value of the midpoint of the first trough and crest is selected as the threshold. Since all the light probes are captured in specific lighting environment, the energy histogram is established using the intensity samples of all the light probes. Figure 7 (b) shows the ordinary image which is rectified for display and the division of the image into two parts using the threshold is shown in Figure 7 (c).

4.4. Rendering

A customized plug-in in open source PBRT (physical based ray-tracing) is used for rendering. When we estimate the lighting of the direction ω on the point \mathbf{x} , integration must be calculated shown as Equation 5[14].

$$\begin{aligned} L_0(\mathbf{x}, \omega_0) &= \int_{\Omega} L_i(\mathbf{x}, \omega) f_r(\omega_0, \mathbf{x}, \omega) \langle \mathbf{n}(\mathbf{x}), \omega \rangle d\omega \end{aligned} \quad (5)$$

Where $L_0(\mathbf{x}, \omega_0)$ stands for outgoing lighting to estimate, and $L_i(\mathbf{x}, \omega)$ refers to the incident lighting in various direction. Function $f_r(\omega_0, \mathbf{x}, \omega)$ is the bidirectional reflection distribution function. Symbol $\mathbf{n}(\mathbf{x})$ is the normal of the plane, to which the \mathbf{x} belongs. In practice, the continuous equation is converted to the sum of several discrete formulas in Equation 6.

$$\begin{aligned} L_0(\mathbf{x}, \omega_0) &= \frac{1}{N} \sum_{n=1}^N L_i(\mathbf{x}, \omega_n) f_r(\omega_0, \mathbf{x}, \omega_n) \langle \mathbf{n}(\mathbf{x}), \omega_n \rangle \end{aligned} \quad (6)$$

In order to calculate the $L_0(\mathbf{x}, \omega_0)$ in the equation, we divide it into two parts $L_i^{\text{direct}}(\mathbf{x}, \omega_0)$ and $L_i^{\text{indirect}}(\mathbf{x}, \omega_0)$ which correspond to the two illumination representations presented before. Then lighting in any direction can be resampled using the recorded samples.

5. Experiment Evaluation

We captured the lighting environment of the real scene using the incident light field capturing setup. Our approach was tested based on the real data and the dataset captured by [6] for comparison. As to the accuracy of the virtual plane position estimation, Table 1 shows the comparison between the real and estimated geometric measures. The result shows our method can correctly capture the position of direct lights in the real scene.

Table 1. Illumination Distribution Estimation Error

Scene	Estimate Count	Lights Position	Estimate Error
Five Area Lights	5	(-376 15026)	18.63
		(-203 150 26)	17.77
		(-33 150 26)	14.30
		(-376 150 270)	27.66
		(-33 150 270)	20.10
Single Point Light	1	(-105 83 23)	9.68

Figure 8(b) is our rendering result directly using the light probe sequence captured by [6], shown as Figure 8(a). Based on his lighting data, we construct the non-uniform illumination representations and use them to illuminate a new virtual scene. Other than the triangular shadow and the bright spot in the center, the shadow border is more smoothly.

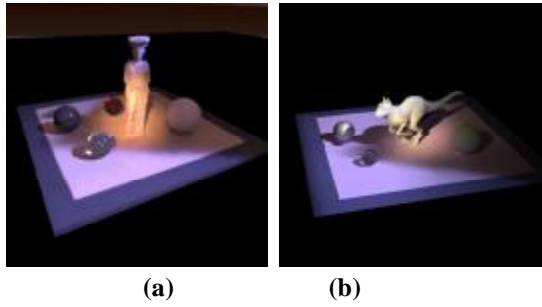


Figure 8.(a)Unger J. et al' rendering result (b)our rendering result by the same light probe sequence

In the second experiment, we place a bonsai between the point light source and the capturing setup. Definitely the bonsai produces particularly sharp shadow on the capturing plane. We apply the adaptive capturing of the incident light field and use this highly spatially varying lighting data to illuminate a virtual Buddha and a silver virtual sphere on the plane. It is clearly that shadows on the plane represent the shape of leaves in Figure 9(b). Meanwhile the rendering result by only one light probe captured in the real-scene is shown in Figure 9(a) for comparison. We cannot see any detail of shadow of the bonsai on the plane.

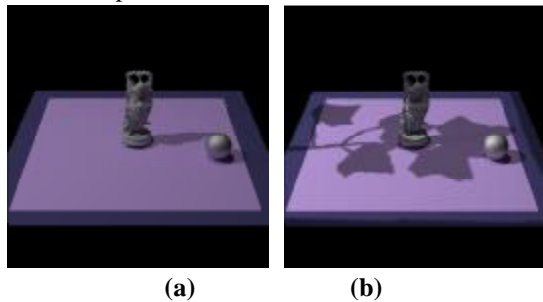


Figure9.(a)the rendering result by one light probe (b) the rendering result using the non-uniform illumination representations

In the third experiment, we capture light probe sequences of the laboratory room and put part of them in a larger image, shown as Figure 10(a).Then, we apply direct illumination and indirect illumination representations to this light data and use this light data to illuminate the virtual scene consisting of five virtual spheres with a variety of materials and four black matte twists. The rendering result is shown as Figure 10(b) which shows highly realistic rendering effect.

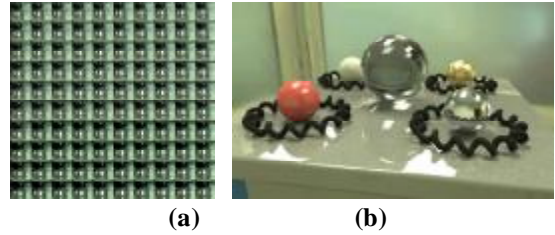


Figure10.(a)raw light probe sequences (b) the rendering result using the direct illumination and the indirect illumination

6. Conclusion

A method is presented in this paper to represent the complicated illumination in the real-world from HDR light probe sequences. The illumination representations employ non-uniform structure instead of uniform light field to simulate spatially and angularly varying lighting. The captured illuminations are divided into direct and indirect parts that are modeled respectively. The non-uniform representations presented in this paper can accurately preserve the spatially and directionally feature of the real lighting. Compared with the traditional illumination representation, it can be integrated to most global illumination algorithms directly. Experiment results illustrated that the non-uniform representation can produce more photo-realistic rendering effects.

Acknowledgment

This work is supported by the National 863 Program of China under Grant No.2012AA011803, the Natural Science Foundation of China under Grant No.61170188, and the National 973 Program of China under Grant No. 2009CB320805.

References

- [1] Heidrich W., Kautz J., Slusallek P., Seidel H. P. Canned light sources. Proceedings of the EG Rendering Workshop 1998, pp. 293–300.
- [2] Goesele M., Granier X., Heidrich W., Seidel H. P. Accurate light source acquisition and rendering. ACM SIGGRAPH 2003 Papers, ACM, pp. 621–630.
- [3] Ihrke I., Stich T., Gottschlich H., Magnorm, Seidel H. P. Fast incident light field acquisition and rendering. Journal of WSCG 16, 1-3 (2008):25–32.
- [4] Mas A., Martín I., and Patow G. Compression and importance sampling of near-field light sources. Computer Graphics forum 2008, Issue 8:2013-2027.
- [5] Zhao Q.P. Data acquisition and simulation of natural phenomena. Sci China Inf Sci, 2011, 54(4):683–716.
- [6] Unger J., Wenger A., Hawkins T., Gardner A., Debevec P. Capturing and rendering with incident light fields. Proceedings of the EG Rendering

Workshop 2003, Eurographics Association, pp. 141–149.

- [7] Unger J., Gustavson S., Larsson P., and Ynnerman A. Free form incident light fields. *Computer Graphics Forum (Proceedings EGSR 2008)*, 27(4):1293–1301.
- [8] J. Low, A. Ynnerman, P. Larsson, and Unger J. HDR light probe sequence resampling for realtime incident light field rendering. *SCCG (Spring Conference for Computer Graphics)*, 2009.
- [9] Mury A.A., Pont S.C., Koenderink J.J. Representing the Light Field in Finite 3D Spaces from Sparse Discrete Samples. *Applied Optics*, 2008.
- [10] Sato I., Sato Y., Ikeuchi K. Acquiring a radiance distribution to superimpose virtual objects onto a real scene. *IEEE Transactions on Visualization and Computer Graphics* 5, 1 (January-March 1999):1–12.
- [11] Corsini, M., Callieri, M., and Cignoni, P. Stereo light probe. *Computer. Graph. Forum* 2008, 27, 2, pp. 291–300.
- [12] Y. Furukawa, B. Curless, S. M. Seitz and R. Szeliski Manhattan world stereo, *IEEE Conference on Computer Vision and Pattern Recognition*, 2009.
- [13] Xu Zhao, Zhong Zhou, Wei Wu. Radiance-based color calibration for image-based modeling with multiple cameras. *Sciences China Information Sciences*, 2012, 55(7):1509-1519.
- [14] Kajiya J. T. The rendering equation. *Computer. Graphics (ACM SIGGRAPH 1986)*, 20(4):143–150.
- [15] Paul E. Debevec and Jitendra Malik. Recovering high dynamic range radiance maps from photographs. *ACM SIGGRAPH* 1997